

Design and implementation of the monochromator shielding for the cold neutron spectrometers XINGZHI and BOYA

Jinchen Wang(汪晋辰), Juanjuan Liu(刘娟娟), Daye Xu(徐大业), Florian Grünauer, Lijie Hao(郝丽杰), Yuntao Liu(刘蕴韬), Hongxia Zhang(张红霞), Peng Cheng(程鹏), and Wei Bao(鲍威)

Citation: Chin. Phys. B, 2024, 33 (**5**): 057801. DOI: 10.1088/1674-1056/ad3629
Journal homepage: http://cpb.iphy.ac.cn; http://iopscience.iop.org/cpb

What follows is a list of articles you may be interested in

Incommensurate-commensurate magnetic phase transition in double tungstate $Li_2Co(WO_4)_2$

Xiyu Chen(陈西煜), Ning Ding(丁宁), Meifeng Liu(刘美风), Tao Zou(邹涛), V. Ovidiu Garlea, Jingwen Gong(龚婧雯), Fei Liu(刘飞), Yunlong Xie(谢云龙), Lun Yang(杨伦), Shuhan Zheng(郑书翰), Xiuzhang Wang(王秀章), Shuai Dong(董帅), T. Charlton, and Jun-Ming Liu(刘俊明)
Chin. Phys. B, 2022, 31 (**4**): 047501. DOI: 10.1088/1674-1056/ac3818

Antiferromagnetic interlayer coupling of (111)-oriented $La_{0.67}Sr_{0.33}MnO_3/SrRuO_3$ superlattices

Hui Zhang(张慧), Jing Zhang(张静), Jin-E Zhang(张金娥), Fu-Rong Han(韩福荣), Hai-Lin Huang(黄海林), Jing-Hua Song(宋京华), Bao-Gen Shen(沈保根), Ji-Rong Sun(孙继荣)
Chin. Phys. B, 2019, 28 (**3**): 037501. DOI: 10.1088/1674-1056/28/3/037501

Observation of spin glass transition in spinel $LiCoMnO_4$

Chen Hong (陈红), Yang Xu (杨旭), Zhang Pei-Song (张培松), Liang Lei (梁磊), Hong Yuan-Ze (洪源泽), Wei Ying-Jin (魏英进), Chen Gang (陈岗), Du Fei (杜菲), Wang Chun-Zhong (王春忠)
Chin. Phys. B, 2015, 24 (**12**): 127501. DOI: 10.1088/1674-1056/24/12/127501

A quantum explanation of the magnetic properties of Mn-doped graphene

Lei Tian-Min (雷天民), Liu Jia-Jia (刘佳佳), Zhang Yu-Ming (张玉明), Guo Hui (郭辉), Zhang Zhi-Yong (张志勇)
Chin. Phys. B, 2013, 22 (**11**): 117502. DOI: 10.1088/1674-1056/22/11/117502

Exchange coupling and helical spin order in the triangular lattice antiferromagnet $CuCrO_2$ using first principles

Jiang Xue-Fan(江学范), Liu Xian-Feng(刘先锋), Wu Yin-Zhong(吴银忠), and Han Jiu-Rong(韩玖荣)
Chin. Phys. B, 2012, 21 (**7**): 077502. DOI: 10.1088/1674-1056/21/7/077502

INSTRUMENTATION AND MEASUREMENT

Design and implementation of the monochromator shielding for the cold neutron spectrometers XINGZHI and BOYA

Jinchen Wang(汪晋辰)[1,†], Juanjuan Liu(刘娟娟)[1,†], Daye Xu(徐大业)[1], Florian Grünauer[2], Lijie Hao(郝丽杰)[3], Yuntao Liu(刘蕴韬)[3], Hongxia Zhang(张红霞)[1,‡], Peng Cheng(程鹏)[1,§], and Wei Bao(鲍威)[1,4,5,¶]

[1] *Laboratory for Neutron Scattering and Beijing Key Laboratory of Optoelectronic Functional Materials and MicroNano Devices, Department of Physics, Renmin University of China, Beijing* 100872, *China*

[2] *Physics Consulting, Zorneding* 85604, *Germany*

[3] *China Institute of Atomic Energy, Beijing* 102413, *China*

[4] *Department of Physics, City University of Hong Kong, Kowloon* 999077, *China*

[5] *Center for Neutron Scattering, City University of Hong Kong, Kowloon* 999077, *China*

(Received 27 December 2023; revised manuscript received 16 February 2024; accepted manuscript online 21 March 2024)

An innovative monochromator shielding is designed and implemented for the cold neutron spectrometers XINGZHI and BOYA operated by Renmin University of China at China Advanced Research Reactor. Via Monte Carlo simulations and careful mechanical designs, a shielding configuration has been successfully developed to satisfy safety requirements of below 3 μSv/h dose rate at its exterior, meanwhile fulfilling space, floor load and nonmagnetic requirements. Composite materials are utilized to form the sandwich-type shielding walls: the inner layer of boron carbide rubber, the middle layer of steel-encased lead and the outer layer of borated polyethylene. Special-shaped liftable shielding blocks are incorporated to facilitate a continuous adjustment of the neutron energy while preventing radiation leakage. Our work has demonstrated that by utilizing composite shielding materials, along with the sandwich structure and liftable shielding blocks, a compact and lightweight shielding solution can be achieved. This enables the realization of advanced neutron scattering instruments that provide expanded space of measurement, larger energy and momentum coverage, and higher flux on the sample. This shielding represents the first of its kind in neutron scattering instruments in China. Following its successful operation, it has been subsequently employed by other neutron instruments across the country.

Keywords: neutron scattering, cold neutron spectrometer, monochromator shielding, sandwich shielding structure

PACS: 78.70.Nx, 75.25.–j, 29.30.Hs, 28.20.–v **DOI:** 10.1088/1674-1056/ad3629

1. Introduction

Neutron scattering instruments play significant roles in many research areas, such as physics, chemistry, biology, and engineering. To reduce the radiation levels of neutrons and gamma rays outside the instruments, shielding is crucial in neutron instrumentation. Specifically, the shielding of the crystal monochromator is the bulkiest component in the entire instrument, as it is exposed to the highest neutron flux.[1] Meanwhile, since the crystal monochromator selects neutron energy by varying the Bragg scattering angle, the shielding must be adjustable according to the desired neutron energy. Moreover, there are usually additional requirements that need to be satisfied, depending on the specific instrument details. Thus, it poses significant technical challenges to design and implement the monochromator shielding.

Concrete and steel are commonly used shielding materials for neutron scattering instruments in China and across the world.[2–7] The practical advantages of these materials, such as their widespread availability and well-established manufacturing processes, make them convenient choices for constructing shielding structures. However, there is an increasing demand for more advanced neutron instruments with improved specifications. This necessitates the development of a compact and lightweight shielding system, as it extends the space of measurement, enlarges the energy and momentum coverage, and increases neutron flux on the sample. Additionally, the shielding of the crystal monochromator needs to be movable in coordination with the selected neutron energy. This requires a robust mechanical design to enable the continuous adjustment of the shielding complex. The large volume and heavy weight of concrete and steel have made them less favorable. Shielding structures utilizing composite materials such as borated material for neutron absorption and lead (Pb) for gamma, have been applied in some cold neutron spectrometers such as SPINS at the NCNR, MIRA and DNS at the FRM Ⅱ, FLEXX at the BER Ⅱ, and IN12 at the ILL.[8–11] However, a detail guidance for

[†]These authors contributed equally to this work.

[‡]Corresponding author. E-mail: hxzhang@ruc.edu.cn

[§]Corresponding author. E-mail: pcheng@ruc.edu.cn

[¶]Corresponding author. E-mail: weibao@cityu.edu.hk

© 2024 Chinese Physical Society and IOP Publishing Ltd

such shielding design and implementation, including simulation, choice of materials, key component manufacturing and engineering, is lacking.

Two cold neutron spectrometers, XINGZHI and BOYA, have been constructed in Beijing under the operation of Renmin University of China. XINGZHI is a triple-axis spectrometer with flexible polarization analysis capability,[12] while BOYA is a multiplexing spectrometer featuring multiple analyzer-detector channels. These spectrometers are based at the 60 MW China Advanced Research Reactor (CARR), which is designed to provide a thermal neutron flux of approximately 8×10^{14} n·cm^{-2}·s^{-1}, and to accommodate a cold source installed inside the reflector.[13] Both instruments are stationed at the CARR neutron guide A (CNGA), which consists of a 17 m long curved guide with a cut-off wavelength of 2 Å and a total length of 15.3 m long straight guides. The straight guide has inner cross section that measures 30 mm in width and 150 mm in height. The curved guide prevents direct sight to the reactor source, effectively filters out fast neutrons and gammas from the reactor and delivers only cold and thermal neutrons to the instruments. XINGZHI is positioned at the end of the straight guide, while BOYA is located second-to-last.

For XINGZHI and BOYA, innovative shielding designs are needed to fulfill the following requirements. (i) The radiation level at the exterior of the shielding should be kept below a dose rate of 3 μSv/h to ensure safety and minimize radiation interference with nearby instruments. (ii) The shielding has to be tunable in coordination with varying neutron energy. (iii) The shielding must be compact to provide sufficient space for continuous neutron energy adjustment from 2.5 meV to 19 meV. (iv) The shielding needs to accommodate a short monochromator-to-sample distance, ranging from 1.5 m to 1.9 m, to enable a higher neutron flux onto the sample. (v) It is essential for the shielding to be nonmagnetic, enabling the performance of high magnetic field experiments. (vi) Finally, the maximum allowed floor loading of 7 t/m^2 needs to be complied.

Here the Monto Carlo simulation is used to guide the shielding designs. A sandwich structure including 3 mm boron carbide (B_4C) rubber, 180 mm lead (Pb) and 100 mm borated polyethylene (BPE) is achieved. Compared with single-material structure such as steel, this sandwich design is superior in both space and weight, and fulfills all instrumental requirements. This is incorporated with a robust mechanical design with special-shaped liftable shielding blocks that facilitate continuous change of neutron energy. It marks the first implementation of neutron monochromator shielding in China that has the sandwich structure and liftable segments. Being compact and lightweight, the shielding design enables neutron instruments to have larger energy and momentum coverage and higher flux on the sample. The effectiveness of this design has been verified and subsequently adopted by other neutron instruments in China, such as HETU at the China Mianyang Research Reactor.[14] Given its potential to guide future shielding designs in neutron instrumentation, we are motivated to report design details in this paper. Note that almost identical monochromator shielding designs have been adopted for XINGZHI and BOYA, with minor variations based on their locations along the neutron guide. So unless explicitly mentioned, they are not individually distinguished throughout the paper. The following sections will present the Monte Carlo simulations, mechanical designs, results and discussions sequentially.

2. Monte Carlo simulations

2.1. Model

The Monto Carlo code MCNP5 was used to optimize the thickness of shielding materials and evaluate their effectiveness.[15] The fluence-to-dose conversion factors for neutrons and photons according to the ICRP Publication 74 were used.[16] To simulate the neutron beam, a virtual neutron source was placed inside the guide, located 700 mm upstream of the monochromator. A homogeneous area distribution within the inner cross section of the guide and an isotropic angular divergence of 0.9° were assumed for the virtual source. The total neutron flux of 7.07×10^9 n·cm^{-2}·s^{-1} and the wavelength distribution of the source were determined from McStas simulations based on the current design of the cold source of CARR.[13]

The schematic model for the Monte Carlo simulation of the monochromator shielding is depicted in Fig. 1. Highly oriented pyrolytic graphite (HOPG) crystals with a thickness of 2 mm (Panasonic Corporation, Japan) are used for the monochromator. The HOPG crystals are mounted on 2 mm-thick boron carbide (B_4C) plates, which are supported by the 5 mm-thick aluminum frame. The monochromator center is positioned 180 mm away from the exit of the neutron guide. A cylindrical shielding is designed with a minimum inner cavity of 250 mm in radius and 500 mm in height. A gap on the shielding cylinder serves as the outlet for the monochromated outgoing neutron beam.

The generation and scattering of neutrons and gammas from the monochromator materials (Al, B_4C and HOPG) are the primary sources of radiation. To effectively shield against neutrons, boron carbide is chosen as the inner shielding material as it only generates secondary photons of 0.48 MeV through the neutron capture reaction ^{10}B(n,α)^{7}Li. In our model, we applied a 3 mm-thick layer of boron carbide rubber with a B_4C concentration of 0.9 g/cm^3 to the inner surfaces of the shielding. Then, additional materials that can absorb

gamma rays and/or neutrons were explored. The evaluations and comparisons of these materials are presented in the following sections.

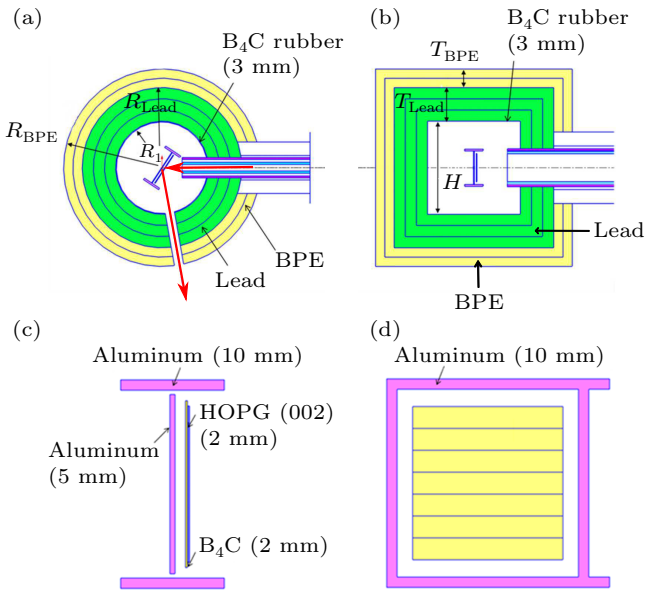


Fig. 1. The schematic model for the Monte Carlo simulation. (a) Horizontal and (b) vertical view of the monochromator shielding model. The paths of the neutron beam from the guide to the monochromater, and from the monochromater to the sample position are indicated by red arrows in panel (a). The inner monochromator space has radius R_1 (250 mm) and height H (500 mm). The radius (R) and thickness (T) of shielding materials, varied in simulations, are labeled in the figures. (c) Horizontal and (d) vertical view of the crystal monochromator model. Highly oriented pyrolytic graphite (HOPG) crystals of 2 mm thickness are mounted on the backplates (2 mm boron carbide for XINGZHI or 1 mm Si for BOYA) supported by the aluminum frame.

2.2. Steel as the shielding material

Concrete was deliberately disregarded due to its significant space requirements. Steel takes less space and is also a widely accessible shielding material. To evaluate the performance of steel, simulations were conducted using stainless steel with various thicknesses ranging from 120 mm to 400 mm. There are no photoneutrons (fast neutrons) generated in stainless steel due to the high gamma-energy-threshold for the photonuclear-effect in iron. Hence the dominant radiation component outside the shielding is gamma radiation. In order to maintain the gamma radiation level below 3 μSv/h outside the shielding, a minimum thickness of 350 mm is required. This results in a total weight of 9.9 t, which exceeds the floor load limit. Therefore, it is necessary to explore more efficient shielding materials that can provide the desired level of radiation protection while reducing the overall space and weight of the shielding.

2.3. Lead as the shielding material

Lead (Pb) is proposed as the next shielding material for gamma radiation. The simulated dose rates of gamma and neutron radiation in the vicinity of the monochromator area

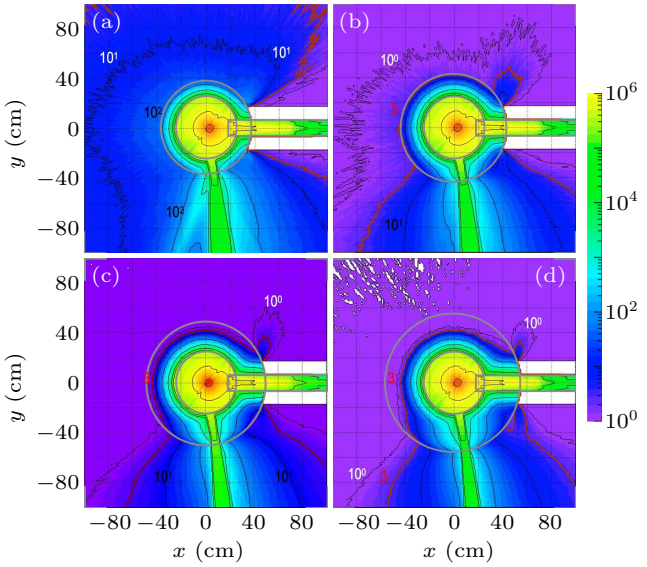


Fig. 2. Distribution of the total gamma dose rate for various lead (Pb) thicknesses of (a) 120 mm, (b) 180 mm, (c) 240 mm and (d) 300 mm. The contour line in red represents the dose rate of 3 μSv/h. The color bar denotes the radiation dose rate in units of μSv/h.

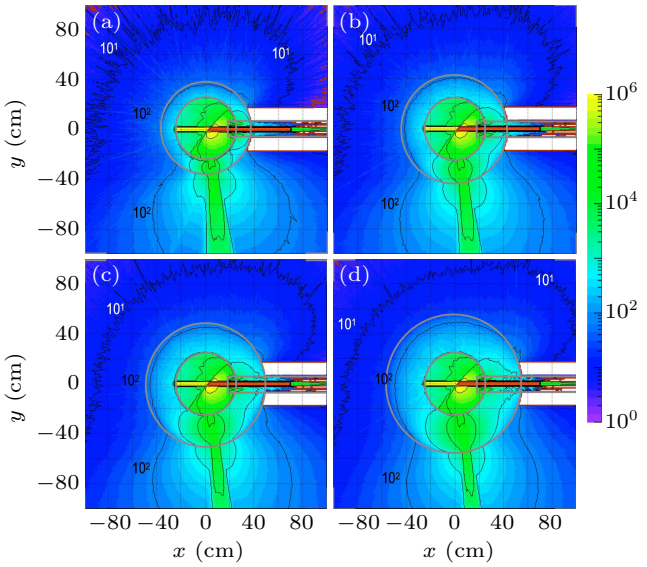


Fig. 3. Distribution of the total neutron dose rate for various lead (Pb) thicknesseses of (a) 120 mm, (b) 180 mm, (c) 240 mm and (d) 300 mm. The color bar denotes the radiation dose rate in units of μSv/h.

for various Pb thicknesses are shown in Figs. 2 and 3, respectively. In Fig. 2, the red line represents the 3 μSv/h limit. It can be seen that the reduction of gamma radiation is obvious when the Pb thickness increases from 120 mm to 180 mm. Beyond 180 mm, most areas outside the shielding remain below the 3 μSv/h, except for the region surrounding the beam outlet where the gamma dose rate reaches approximately 10 μSv/h. This will be addressed later in the mechanical designs section. Further increasing the Pb thickness beyond 180 mm does not provide significant benefits. Hence a 180 mm layer of Pb is deemed to provide a sufficient gamma shielding. Compared to stainless steel, Pb requires a lower thickness (180 mm) and less weight (4.56 t), making it a superior choice. However, the neutron dose rate ranges from 10 μSv/h to 100 μSv/h (see

Fig. 3), which exceeds the requirement of 3 μSv/h. This is mainly attributed to the photonuclear effect of (γ, n) reactions in Pb. These reactions have a low gamma-energy-threshold (6.7 MeV) and generate fast neutrons. The simulations indicate that neutrons with energies above 0.1 MeV dominate the dose rate outside the shielding.

2.4. Lead and polyethylene as the shielding material

As Pb generates secondary fast neutrons, it is considered to incorporate additional materials to slow down and shield fast neutrons. Polyethylene is an excellent neutron moderator due to its high concentration of hydrogen and lightweight. And boron is widely used for absorbing thermal neutrons. So borated polyethylene (BPE) with 5 wt.% B_2O_3 is considered as an extra layer of shielding material outside the Pb.

Figures 4 and 5 present the calculated distribution of neutron and gamma dose rates when incorporating an additional layer of BPE in thicknesses of 50 mm, 100 mm and 150 mm outside the 180 mm Pb shielding. As shown in Fig. 5, the inclusion of BPE substantially reduces the neutron dose rate. To achieve a neutron dose rate below 3 μSv/h outside the shielding, a thickness of up to 100 mm is necessary. On the other hand, the gamma level has a slight increase due to the (n, γ) reactions occurring in the BPE. Fortunately, the gamma dose rate remains below the 3 μSv/h threshold.

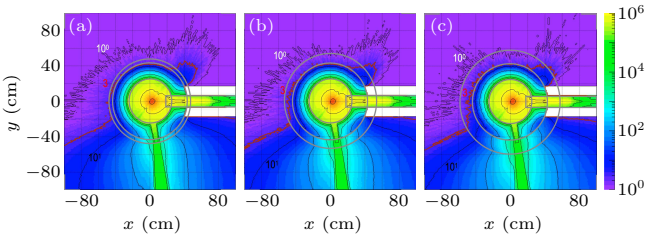


Fig. 4. Distribution of total gamma dose rate for various borated polyethylen thicknesses (as outer shielding layer) of (a) 50 mm, (b) 100 mm and (c) 150 mm outside the 180 mm Pb sheilding. The contour line in red represents the dose rate of 3 μSv/h. The color bar denotes the radiation dose rate in units of μSv/h.

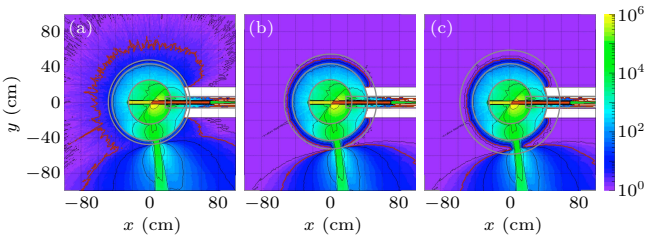


Fig. 5. Distribution of total neutron dose rate for various borated polyethylen thicknesses (as outer shielding layer) of (a) 50 mm, (b) 100 mm and (c) 150 mm outside the 180 mm Pb sheilding. The contour line in red represents the dose rate of 3 μSv/h. The color bar denotes the radiation dose rate in units of μSv/h.

As a result, the sandwich shielding wall comprising an inner layer of 3 mm boron carbide rubber, a middle layer of 180 mm Pb and an outer layer of 100 mm BPE is designed for our monochromator shielding. The total mass of the sandwich cylinder amounts to 4.99 t, and the total thickness is 280 mm. It is significantly thinner and lighter, compared with the 9.9 t and 350 mm steel shielding cylinder. All three materials used in the shielding are nonmagnetic. This design successfully meets the radiation protection requirements while satisfying additional criteria including spatial constraints, floor load limits, and the need for nonmagnetic materials.

3. Mechanical designs

The design view of the monochromator shielding is shown in Fig. 6. The shielding consists of both stationary shielding blocks and liftable shielding blocks, along with the beam limiter group, the beam catcher (for XINGZHI only) and ground supporters. As seen in the horizontal view in Fig. 6(b), the shielded house exhibits a rectangular region measuring 270 mm × 540 mm enclosed by stationary shielding blocks, and a semi-circular region with a radius of 292.5 mm, enclosed by both stationary and liftable shielding blocks. The shielding complex accommodates the crystal monochromator in the center, which is aligned to the beam with an accuracy within 1 mm, and 180 mm away from the end of the neutron guide. The lower portion of the housing space extends 480 mm below the beam level, providing room for monochromater stages, including motorized goniometers and positioning stages. The upper portion extends 155 mm above the beam level, offering space for the optional magnet guide field for polarized neutron experiments (Figs. 6(c) and 6(d)).

Both stationary and liftable shielding blocks are constructed with three layers as recommended by the Monte Carlo calculations: 5 mm-thick B_4C rubber on the internal surfaces, Pb layer encased in a stainless steel can in the middle, and 100 mm-thick BPE on the outside. The Pb-steel structure is manufactured by pouring liquid Pb into stainless steel cans, which are internally reinforced with ribs in the circumferential direction. This produces defect-free, space-saving, and engineering friendly Pb shielding blocks. The dimensions of the Pb layer vary slightly between the stationary and liftable blocks. For the stationary block, the Pb layer is 175 mm in thickness encased in a 10 mm-thick stainless steel can. For the liftable block, the Pb layer is 180 mm in thickness encased in a 2.5 mm-thick stainless steel can. The stationary shielding consists of six blocks that are connected via stepped joints, creating labyrinth-type gaps to minimize radiation leakage. The tolerances for the male and female stepped joints are −0.5 mm to 0 and 0 to 0.5 mm, respectively. Consequently, the labyrinth gap size ranges from 0 to 1 mm between adjacent blocks with no direct line-of-sight paths through the shielding.

The 14 liftable shielding blocks are specially shaped and collectively cover an arc of 126°. As illustrated in Figs. 7(a) and 7(b), each individual block covers 9° with step joints spanning 1.75° on each side. This configuration allows for a win-

dow opening of 7.25° when a single block is lifted. The tolerance for the mating edges shall be within 0.05°. Radially, there is a 7 mm gap in the Pb layer between the mating blocks, filled with 5 mm-thick B_4C rubbers, and a similar 2 mm gap in the BPE layer. These create labyrinthine gaps with the size of 2 mm radially and 0–0.5 mm tangentially. Each liftable block has a weight of 60 kg and can be raised up to 250 mm using a commercial pneumatic cylinder (Festo (China) Ltd., Model DNC-5-250-PPV-ELH) and a pair of parallel guide rods, as shown in Fig. 7(a).

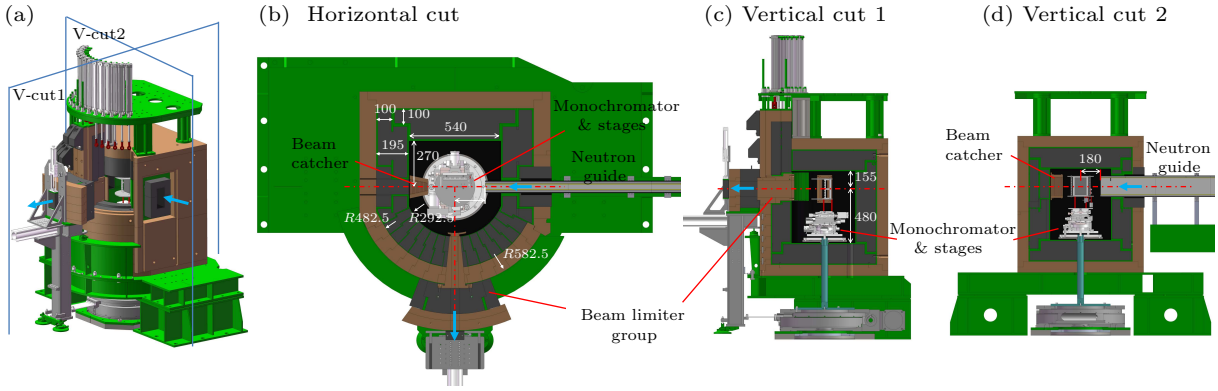


Fig. 6. Design diagram of the monochromator shielding in (a) 3D perspective, (b) horizontal cut, (c) and (d) vertical cuts. The horizontal cut is at the beam level, and the directions of two vertical cuts are indicated in panel (a). The monochromator and its stages, beam limiter group and beam catcher (for XINGZHI only) are denoted. The beam level is represented by red dash lines, while the incoming and outcoming neutron beams are depicted by blue arrows. The key distances and radii are marked with white numbers, in units of mm.

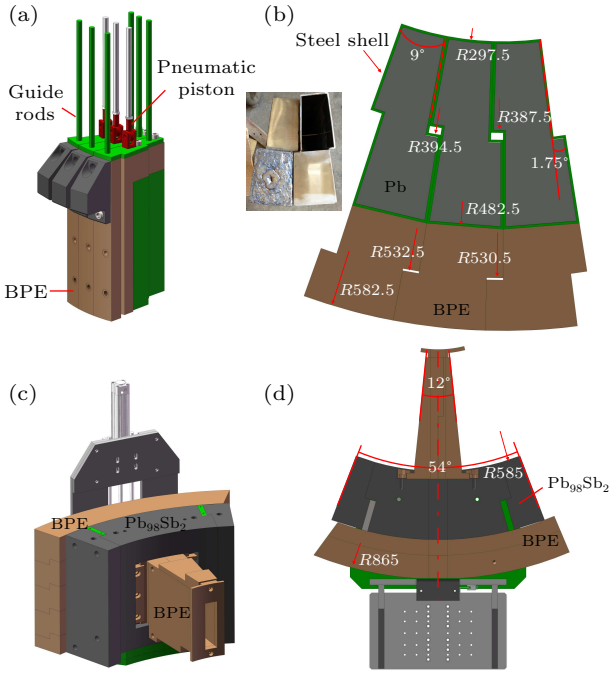


Fig. 7. (a) Design diagram of the liftable shielding blocks and (b) the horizontal cut. The actual photo of two steel-encased Pb blocks is shown in the inset. (c) Design diagram of the beam limiter group and (d) the horizontal cut. The lead and borated polyethylene are denoted by Pb and BPE, respectively. The key distances and radii are marked by white numbers, in units of mm.

The Monte Carlo results in the previous section reveal that the dose rates are high around the beam outlet. To further reduce the radiation level around the outgoing beam path, a beam limiter group is introduced. As depicted in Figs. 7(c) and 7(d), the group consists of a BPE beam limiter and fan-shaped shielding blocks made of $Pb_{98}Sb_2$ and BPE. The BPE beam limiter is a 12° tunnel that is inserted into the beam outlet to transport and limit the neutron beam. It is surrounded by a 180 mm-thick $Pb_{98}Sb_2$ block and an outer layer of 100 mm-thick BPE. Here the $Pb_{98}Sb_2$ layer serves the same purpose as the Pb layer in the stainless steel can. $Pb_{98}Sb_2$ is mechanically stronger and easier for manufacturing than pure Pb thus does not need the additional stainless steel encasement. Noted that Sb may cause a higher activation and therefore a higher delayed gamma dose rate after irradiation, we have limited the use of $Pb_{98}Sb_2$ only in the beam limiter group, which is relatively far away from the monochromator. Both $Pb_{98}Sb_2$ and BPE shielding blocks cover an arc of 54°, equaling to the total angle of six liftable blocks. Step joints on their surfaces mate with adjacent liftable and stationary shielding blocks, forming labyrinth gaps to minimize radiation leakage. The group is positioned on the axis connecting the monochromator to the sample, and can be rotated by the rotation stage synchronously with the rotation of the take-off angle of the monochromator. Thus when the desired neutron energy is selected at the monochromator, 2 to 3 liftable blocks are elevated to open an outlet window, and the beam limiter group is appropriately rotated to shield the surrounding area. If needed, Söller collimators can be installed inside the group for further collimating the outgoing beam.

The entire monochromator shielding with a total weight of 8550 kg is mounted on a stainless steel bridge with two supports. The deformation and stress of the bridge are critical for the rotation of the beam limiter group and the overall success of the shielding complex. To ensure its structural integrity and optimize the engineering design, finite element modeling has been employed on the bridge and the two supports. The bridge measured 2.22 m in length, 1.05 m in width and 0.56 m

in height from the floor. The optimized thicknesses of the plate and the ribs are 20 mm and 15 mm, respectively. As shown in Fig. 8, the maximum stress is 19 MPa, which is well below the allowed ultimate yield strength. And the maximum deformation is 0.07 mm, which satisfies the design requirements. Two air pads on the arc plate of the bridge can stably support the beam limiter group and move smoothly when changing the monochromated neutron energy. It is noted that the simulated stress and deformation can be further reduced by adding chamfers and fillets to the model, which are employed during the practical design and manufacturing of the rib parts.

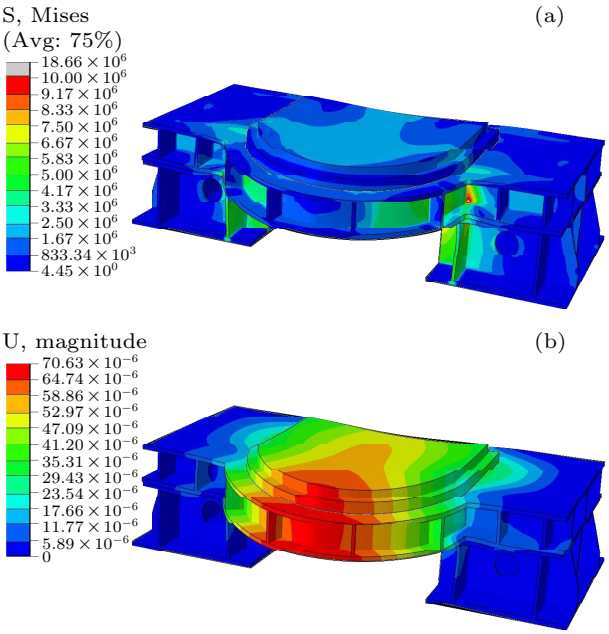


Fig. 8. (a) The Mises stress in the unit of Pa and (b) deformation in the unit of m contoured on the bridge and the two supports simulated from the finite element analysis. To better show the deformation, the structure is deformed by a scale factor of 1000.

4. Result and discussion

During implementation, many engineering challenges have been overcome. For example, the borated composite materials, boron carbide rubber and borated polyethylene, were not readily available. Through the collaborative research and development effort with domestic manufacturers, these materials have been stably produced and supplied. Furthermore, Pb is too soft for drilling and fastening. The utilization of steel-encased Pb and $Pb_{98}Sb_2$ alloy has enabled space-saving and engineering friendly Pb layers. Additionally, the liftable block has undergone meticulous design considerations, including its irregular shape and tolerances, to ensure the reliable motion with neutron energy, and to form the labyrinth gaps that minimize the radiation leakage. The successful resolutions of these engineering challenges are crucial in bringing the shielding design to realization. And in the process, we have cultivated domestic manufacturers with expertise in neutron instrument shielding engineering.

Here, the photos of constructed monochromator shielding for BOYA are provided. In Fig. 9(a), the crystal monochromator including Al frames and motorized stages can be seen in the center of the shielded space. The three layer B_4C/Pb/BPE shielding structure with step joints and labyrinthine gaps is visible. The beam limiter group that shields around the outgoing beam is presented in Fig. 9(b), where two of the fourteen liftable blocks are raised to allow the passage of the selected neutrons. A shutter is placed outside the outlet, which is not shown in the photos.

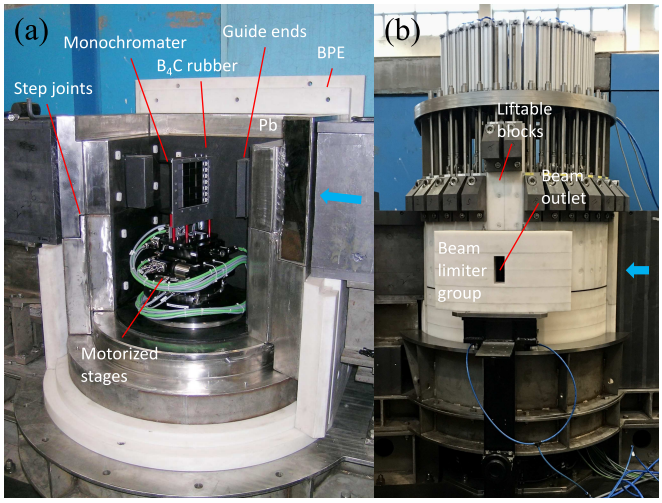


Fig. 9. The photographs illustrate the BOYA monochromator shielding during its construction, showing (a) the partially installed and (b) the fully assembled configuration. Key components are labeled for reference. The blue arrow indicates the direction of the neutron beam in the neutron guide.

There are slight variations of the monochromator designs for XINGZHI and BOYA instruments, based on their position along the neutron guide. XINGZHI is located at the end of the guide while BOYA is upstream of XINGZHI. Consequently, at XINGZHI, most neutrons are stopped within the monochromator shielding, whereas at BOYA, most neutrons exit the monochromator shielding through the outgoing guide. Therefore, a 2 mm B_4C plate is used to back the HOPG (see Fig. 1(c)) at XINGZHI, whereas a 1 mm Si plate is used at BOYA. Additionally, a beam catcher is used at XINGZHI to absorb the unscattered neutrons at the end of the guide (see Fig. 6(b)) whereas it is unnecessary at BOYA. In terms of radiation effects, the low-energy gamma radiation from neutron capture in boron is decreased at BOYA. However, the high-energy gamma radiation is increased from neutron absorption in Si. We conducted simulations to assess this effect and determined that the current three-layer shielding scheme, B_4C/Pb/BPE, is effective for both instruments.

Upon completion of the construction, we have thoroughly surveyed the gamma and neutron dose rates outside the shielding structure at CARR's routine operation of 30 MW.

The gamma dose rate is predominantly distributed around 0.5 μSv/h, varying depending on the specific location of the measurement. The neutron dose rate is weaker and below 0.2 μSv/h at all our recorded locations. All together, the radiation level satisfies the safety requirements and there is sufficient margin even when CARR runs at its maximum power of 60 MW in the future.

After years of operation, the sandwich structure utilizing composite shielding materials B_4C/Pb/BPE, along with the implementation of pneumatic liftable shielding blocks, has proven to be successful. All safety and instrumentation requirements are fulfilled. The positive outcomes validate the effectiveness of the design and implementation of the monochromator shielding, which includes Monte Carlo simulations, mechanical designs, material manufacturing and processing methods, and the construction work. Subsequently, this shielding design has been adopted by HETU instruments at the China Mianyang Research Reactor.[14]

5. Conclusion

The monochromator shielding for cold neutron spectrometers XINGZHI and BOYA at China Advanced Research Reactor has been successfully designed and implemented. During the design process, not only the secondary gamma radiation from (n, γ) reactions but also secondary fast neutron radiation from the photonuclear effect of (γ, n) reactions should be taken into account. To effectively address the combined tasks of neutron moderation, absorption, and gamma attenuation, the three-layer sandwich shielding structure is achieved, consisting of B_4C rubber, Pb, and borated polyethylene. Composed of stationary and liftable shielding blocks and beam limiter groups, the shielding configuration is adjustable according to the desired neutron energy. The design with composite materials is superior to single material structure such as concrete and steel. The compact shielding structure not only effectively reduces radiation levels, but also contributes to a larger energy and momentum coverage and higher neutron flux. This shielding, incorporating a sandwich three-layer structure and liftable segments, represents the first of its kind and a pioneering development among neutron instruments in China. As there is an increasing number of proposals for neutron spectrometers, we believe that our successful design and implementation of this shielding system will contribute to the advancement of neutron instrumentation.

Acknowledgments

Many people contributed to the design and implementation of the monochromator shielding for XINGZHI and BOYA instruments. The authors are particularly indebted to Junfeng Li and Wenwei Shen for their contributions to engineering implementation. The authors also gratefully acknowledge the help of Dr. P. Link from Heinz Maier-Leibnitz Zentrum, Technische Universität München, and Dr. A. Schneidewind from the Jülich Center for Neutron Science (JCNS), Forschungs Zentrum Jülich GmbH, and Dr. K. Habicht from Helmholtz-Zentrum Berlin für Materialien und Energie Gmbh, Berlin. Project supported by the National Natural Science Foundation of China (Grant Nos. 12004426, U2030106, and 12304185), the National Key Scientific Instrument and Equipment Development Project of NSFC (Grant No. 11227906), and the National Key R&D Program of China (Grant No. 2023YFA1406500).

References

[1] Shirane G, Shapiro S M and Tranquada J M 2002 *Neutron Scattering With a Triple-Axis Spectrometer Basic Techniques* (Cambridge: Cambridge University Press)

[2] Gao J, Li J, Li J, Liu Y and Chen D 2010 *China J. Mech. Eng.* **21** 275

[3] Liang T R, Shen F, Yin W, Yu Q Z, Yu C X, Tao J Z and Liang T J 2014 *Chin. Phys. C* **38** 078202

[4] Shen F, Liang T R, Yin W, Yu Q Z, Zuo T S, Yao Z E, Zhu T and Liang T J 2014 *Acta Phys. Sin.* **63** 152801 (in Chinese)

[5] Pyka N, Noack K and Rogov A 2002 *Appl. Phys. A* **74** s277

[6] Danilkin S, Horton G, Moore R, Braoudakis G and Hagen M 2007 *J. Neutron Res.* **15** 55

[7] Yılmaz E, Baltas H, Kırıs E, Ustabas İ, Cevik U and El-Khayatt A 2011 *Ann. Nucl. Energy* **38** 2204

[8] Georgii R, Weber T, Brandl G, Skoulatos M, Janoschek M, Mühlbauer S, Pfleiderer C and Böni P 2018 *Nucl. Instrum. Methods Phys. Res. Sect. A* **881** 60

[9] Skoulatos M and Habicht K 2011 *Nucl. Instrum. Methods Phys. Res. Sect. A* **647** 100

[10] Grünauer F, Keller T, Georgii R, Hertwig M and Skoulatos M 2023 *Nucl. Instrum. Methods Phys. Res. Sect. A* **1047** 167854

[11] Schmalzl K, Schmidt W, Raymond S, Feilbach H, Mounier C, Vettard B and Brückel T 2016 *Nucl. Instrum. Methods Phys. Res. Sect. A* **819** 89

[12] Cheng P, Zhang H, Bao W, Schneidewind A, Link P, Grünwald A, Georgii R, Hao L and Liu Y 2016 *Nucl. Instrum. Methods Phys. Res. Sect. A* **821** 17

[13] Chen D, Liu Y, Gou C and Ye C 2006 *Physica B* **385** 966

[14] Wang B, Zhong S, Lin H, Li J, Yang Z, Goukassov A, Zhang H and Sun G 2023 *J. Appl. Crystallogr.* **56** 1485

[15] Josey C J and Sood A 2023 *A Review of 70 Years of Monte Carlo Development at Los Alamos:* 1953–2023

[16] ICRP 1996 *ICRP Publication* 74. *Ann. ICRP* **26**